



Measurement report: Characteristics of nitrogen-containing organics in PM_{2.5} in Ürümqi, northwestern China – differential impacts of combustion of fresh and aged biomass materials

Yi-Jia Ma^{1,2}, Yu Xu², Ting Yang^{1,2}, Hong-Wei Xiao², and Hua-Yun Xiao²

¹School of Environmental Science and Engineering, Shanghai Jiao Tong University, Shanghai 200240, China

²School of Agriculture and Biology, Shanghai Jiao Tong University, Shanghai 200240, China

Correspondence: Yu Xu (xuyu360@sjtu.edu.cn)

Received: 28 October 2023 – Discussion started: 4 January 2024

Revised: 14 March 2024 – Accepted: 15 March 2024 – Published: 15 April 2024

Abstract. Nitrogen-containing organic compounds (NOCs) are abundant and important aerosol components deeply involved in the global nitrogen cycle. However, the sources and formation processes of NOCs remain largely unknown, particularly in the city (Ürümqi, China) farthest from the ocean worldwide. Here, NOCs in PM_{2.5} collected in Ürümqi over a 1-year period were characterized by ultra-high-resolution mass spectrometry. The abundance of CHON compounds (mainly oxygen-poor unsaturated aliphatic-like species) in the positive ion mode was higher in the warm period than in the cold period, which was largely attributed to the contribution of fresh biomass material combustion (e.g., forest fires) associated with amidation of unsaturated fatty acids in the warm period, rather than the oxidation processes. However, CHON compounds (mainly nitro-aromatic species) in the negative ion mode increased significantly in the cold period, which was tightly related to aged biomass combustion (e.g., dry straws) in wintertime Ürümqi. For CHN compounds, alkyl nitriles and aromatic species showed higher abundance in the warm and cold periods, respectively. Alkyl nitriles can be derived from fresh biomass material combustion associated with the dehydration of amides (the main CHON compounds in the warm period). In contrast, aromatic species were tightly related to aged biomass burning. These findings further suggested different impacts of the combustion of fresh and aged biomass materials on NOC compositions in different seasons. The overall results shed light on the mechanisms by which fresh and aged biomass materials release different NOCs during combustion.

1 Introduction

Fine particulate matter (PM_{2.5}) is a typical atmospheric pollutant that can affect the global climate system, as well as urban air quality and human health (Seinfeld et al., 2016; K. Wang et al., 2021). Organic aerosol (OA) contributes significantly (20 %–90 %) to PM_{2.5} mass concentration in most polluted areas worldwide (Zhang et al., 2007; Han et al., 2023). Up to 77 % of molecules in OA include nitrogen-containing functional groups (Ditto et al., 2020; Kenagy et al., 2021), which have been suggested to play important roles in the formation, transformation, acidity, and hygroscopic-

ity of OA (Xu et al., 2020; Y. Wang et al., 2017; Laskin et al., 2009). Moreover, the further oxidation or nitrification of some nitrogen-containing organic compounds (NOCs) and volatile organic compounds (VOCs) by ozone (O₃), hydroxyl radical (•OH), and nitrogen oxides (NO_x) can lead to an increase in the health hazards of OA (Franze et al., 2005; Bandowe and Meusel, 2017). Nitrated amino acids and nitrated polycyclic aromatic hydrocarbons (PAHs) are two representative hazard NOCs (Franze et al., 2005; Bandowe and Meusel, 2017). Thus, the identification of aerosol NOCs at the molecular level is important for improving our under-

standing of the precursors, sources, and formation processes of nitrogen-containing OA.

Previous observations in urban, rural, marine, and forest areas have suggested that the molecular composition and relative abundance of aerosol NOCs were spatially different (Samy and Hays, 2013; Jiang et al., 2022; Lin et al., 2012; Xu et al., 2023; Zeng et al., 2020, 2021; Zhang et al., 2022). These differences can be mainly attributed to the diverse sources and formation mechanisms of aerosol NOCs. Commonly reported primary sources include combustion process releases and natural emissions (e.g., soils, plant debris, pollen, and ocean) (Song et al., 2022; Y. Wang et al., 2017; Cape et al., 2011; Lin et al., 2023). In addition, aerosol NOCs can also be tightly associated with secondary formation processes involving the reactions of reactive nitrogen with VOCs or particle-phase CHO compounds (Bandowe and Meusel, 2017; Zarzana et al., 2012; Laskin et al., 2014). For example, laboratory experiments have found that the oxidation of isoprene and α -/ β -pinene in the presence of NO_x can result in the formation of organic nitrates (e.g., methacryloyl peroxy-nitrate, dihydroxynitrates, and monohydroxynitrates) (Surratt et al., 2010; Rollins et al., 2012; Nguyen et al., 2015). The reduced nitrogen species (e.g., NH₃, NH₄⁺, and organic amines) have been demonstrated to contribute to the formation of NOCs through “carbonyl-to-imine” transformations in the laboratory experiments (Zarzana et al., 2012; Laskin et al., 2014). In the field observation studies, NOCs in particulate matter were analyzed at the molecular level to indicate their sources and formation mechanisms (Jiang et al., 2022; Lin et al., 2012; Zhong et al., 2023). Xu et al. (2023) characterized the variations of molecular compositions in urban road PM_{2.5}, suggesting that organic nitrates increased largely through the interactions of atmospheric oxidants, reactive gas-phase organics, and aerosol liquid water. Several field studies conducted in Beijing (China) and Guangzhou (China) also suggested that the molecular compositions and formation of NOCs were tightly associated with environmental conditions (Jiang et al., 2022; Lin et al., 2012; Xie et al., 2020). Generally, most studies on aerosol NOCs were performed in economically developed regions and in forest and marine areas (Jiang et al., 2022; X. Wang et al., 2017; Ditto et al., 2022b; Altieri et al., 2016; Xu et al., 2020; Liu et al., 2023; Zhang et al., 2022; Zeng et al., 2020). In contrast, few studies have investigated the sources and atmospheric transformation of NOCs in the urban northwestern border regions of China (e.g., Ürümqi), which feature fragile ecology and harsh environmental conditions (e.g., cold winter and dry summer) that may hinder our comprehensive and in-depth understanding of the formation process of NOCs in ambient aerosols.

Biomass burning emissions were widely reported in the source identification of aerosol NOCs in northern and southwestern China because of heating and cooking needs (Zhong et al., 2023; Wang et al., 2021b; Chen et al., 2017). A recent observation study in urban Tianjin suggested that most

CHON compounds in wintertime PM_{2.5} originated from biomass burning (Zhong et al., 2023). The CHN₂ compounds have been identified in biomass burning OA (BBOA) (Laskin et al., 2009; Y. Wang et al., 2017). Moreover, the high temperature generated by biomass burning can facilitate the release of ammonia, a process that caused the reaction of carboxylic acids (e.g., oleic acid) with ammonia to form amides and alkyl nitriles (Radzi Bin Abas et al., 2004; Simoneit et al., 2003). Interestingly, we found that biomass burning in rural China typically includes fresh biomass materials (e.g., forest fires) and aged biomass materials (e.g., straw after autumn harvest, fallen leaves, and deadwood). Fresh biomass is rich in oils and proteins, whereas aged biomass materials are usually oligotrophic due to the transfer of nutrients to tender tissues or fruits (Jian et al., 2016; Xu and Xiao, 2017). Thus, NOCs released from different types of biomass combustion may vary in molecular composition. However, there are large gaps in our current knowledge about the impacts of fresh and aged biomass burning on NOCs in ambient aerosols.

Ürümqi (northwestern China) is the largest inland city (a total area of 14 216 km²) farthest from the ocean in the world, which is becoming increasingly prominent due to the national strategy of the “One Belt, One Road”. The city and neighboring countries have a dry summer that can easily trigger forest fires (Bátori et al., 2018; Xu et al., 2021), while the winter is freezing with intensive aged biomass and fuel combustion for heating (Ren et al., 2017). In this study, we present 1-year ambient measurements of the chemical compositions in PM_{2.5} collected from Ürümqi. The specific aims of this study are (1) to investigate the molecular-level speciation of functionalized organic nitrogen compounds via high-resolution mass spectrometry with positive (ESI+) and negative (ESI-) ionizations and (2) to investigate the potential sources and formation processes for NOCs with a special focus on the relative influences of fresh and aged biomass burning in different seasons.

2 Materials and methods

2.1 Study site description and sample collection

The study was conducted in Ürümqi city, which has an average altitude of 800 m. The region has an arid temperate continental climate with an annual mean temperature of 7.4 ± 13.9 °C and an annual mean rainfall of 27.8 mm. The sampling site is located in the suburban area (Boda campus of Xinjiang University) of the city (43.86° N, 87.75° E) (Fig. S1 in the Supplement), which is characterized by low population and traffic density. This is because Ürümqi is relatively vast and sparsely populated compared to developed coastal cities in China (Qizhi et al., 2016). Additionally, the area is surrounded by mountains on three sides, resulting in the difficulty in diffusing air pollutants. The dominant forest trees in this area are *Picea schrenkiana*, *Betula tianschanica* Rupr., *Populus talassica* Kom., and *Ulmus pumila* L. The dry cli-

mate and strong sunlight in the warm period (18.81 ± 6.4 °C, Table S1 in the Supplement) would be the main culprits of forest fires in the local and nearby areas. In the cold period (-1.96 ± 11.26 °C) (Table S1), the centralized heating and aged biomass burning may be the main contributors to local air pollution. Thus, it provides an unexpected opportunity to investigate the potentially differential impacts of fresh and aged biomass burning on aerosol NOCs.

A high-volume air sampler (Series 2031, Laoying, China) was set up on the rooftop of a building (School of Geology and Mining Engineering, Xinjiang University). PM_{2.5} samples ($n = 73$) were collected every 5 d with a duration of ~ 24 h onto prebaked (450 °C for ~ 10 h) quartz fiber filters (Pallflex, Pall Corporation, USA) from 1 March 2018 to 26 February 2019. One blank filter was collected every month ($n = 12$). All filter samples were stored at -30 °C until further analysis. During the sampling campaigns, the meteorological data (e.g., temperature and relative humidity) and the concentrations of O₃ and NO_x were recorded hourly from the adjacent environmental monitoring station. These hourly data were then averaged to obtain daily values to match the sampling time of PM_{2.5}. In addition, the trajectories (72 h) of air masses arriving at the sampling site at each sampling event were calculated to investigate the potential influence of pollutant transport on aerosol NOCs.

2.2 Chemical analysis

A portion of each filter sample was extracted twice using 3 mL methanol (LC-MS grade, CNW Technologies Ltd.) under sonication in a chilled ice slurry (~ 4 °C). The extracted solutions were filtered through a polytetrafluoroethylene syringe filter (0.22 μ m, CNW Technologies GmbH). Subsequently, the extracts were concentrated to 300 μ L with a gentle stream of gaseous nitrogen (Shanghai Likang Gas Co., Ltd). The final extracts were analyzed using an ultra-performance liquid chromatography quadrupole time-of-flight mass spectrometry equipped with an electrospray ionization (ESI) source (UPLC-ESI-QToFMS, Waters Acquity Xevo G2-XS) in both ESI+ and ESI– modes (Wang et al., 2021a). It should be pointed out that UPLC-ESI-MS (i.e., TOF-only) was used to identify molecular formulas of organic matter, while the functional groups of the target molecule formulas were deciphered by UPLC-ESI-MS/MS (i.e., tandem mass spectrometry). Ions obtained from m/z 50–700 were assigned molecule formulas by assuming hydrogen or sodium adducts in ESI+ mode and deprotonation in ESI– mode. Detailed chromatographic conditions, parameter selection, and quality control were displayed in the Supplement (Sect. S1). Notably, there may be differences in ionization efficiencies between compound types. However, the exact impacts of ionization efficiency on multifunctional compounds in a complex mixture are uncertain and difficult to evaluate (Ditto et al., 2022b; Yang et al., 2023). Thus, the intercomparison across compound relative abun-

dance without considering potentially differentiated ionization efficiency was conducted in this study, which was similar to many previous studies (Xu et al., 2023; Jiang et al., 2022).

For the measurement of inorganic ions, a portion of each filter sample was ultrasonically extracted with Milli-Q water (18 M Ω cm) (3 mL) in an ice-water bath (~ 4 °C). The extract solutions were then filtered via a polytetrafluoroethylene syringe filter (0.22 μ m, Millipore, Billerica, MA). The concentrations of water-soluble inorganic ions, including NO₃[−], SO₄^{2−}, Cl[−], Ca²⁺, Mg²⁺, Na⁺, and NH₄⁺ in the samples were determined using an ion chromatograph system (Dionex Aquion, Thermo Scientific, USA) (Xu et al., 2022a; Lin et al., 2023).

2.3 Compound categorization and predictions of ALW, pH, and hydroxyl radical

The molecular formulas identified by UPLC-ESI-QToFMS were classified into several major compound classes based on their elemental compositions (i.e., C, H, O, and N), primarily including CHO, CHON, and CHN groups in the ESI+ mode and CHO, CHON, CHOS, and CHONS groups in the ESI– mode (Y. Wang et al., 2017). CHOS and CHONS compounds were also detected in the ESI– mode, with numbers of 398 and 112, respectively (Table S2). As this study focused mainly on NOCs, sulfur-containing species were not discussed. Unless stated otherwise, all of the detected molecules were reported as neutral molecules. The double-bond equivalent (DBE) and carbon oxidation state (OS_C) were calculated to reflect the unsaturation degree of the organics and the composition evolution of organics that underwent oxidation processes, respectively (details in Sect. S2) (Kroll et al., 2011; Xu et al., 2023). The identified compounds can be further classified into four subgroups based on the number of carbon atoms and OS_C value (Kroll et al., 2011; Xu et al., 2023). Briefly, semi-volatile oxidized organic aerosol (SV-OOA) and low-volatility oxidized organic aerosol (LV-OOA) were associated with multi-step oxidation reactions, with OS_C values between -1 and $+1$ and molecular formulas less than 13 carbon atoms. BBOA has OS_C values ranging from -0.5 to -1.5 and more than seven carbon atoms. Compounds with OS_C values less than -1 and carbon atoms above 20 may be related to hydrocarbon-like organic aerosol (HOA). Additionally, the modified aromaticity index (AI_{mod}) was also calculated to indicate the aromaticity of organic compounds (details in Sect. S2) (Koch and Dittmar, 2006). The van Krevelen diagrams and AI_{mod} values have been proposed to further classify organic matter categories (Xu et al., 2023; Su et al., 2021), according to which the identified five subgroups included saturated-like molecules (Sa, $H/C \geq 2.0$), unsaturated aliphatic-like molecules (UA, $1.5 \leq H/C < 2.0$), highly unsaturated-like molecules (HU, $AI_{mod} \leq 0.5$ and $H/C < 1.5$), highly aromatic-like molecules (HA, $0.5 < AI_{mod} \leq 0.66$), and polycyclic aromatic-like

molecules (PA, $AI_{\text{mod}} > 0.66$). Furthermore, it has been suggested that the above subgroups can be subdivided into O-poor and O-rich compounds depending on their O/C ratio (Table S8) (Merder et al., 2020; Zhong et al., 2023).

A thermodynamic model (ISORROPIA-II) was applied to predict the mass concentration of aerosol liquid water (ALW) and the value of pH with particle-phase ion concentrations, as well as ambient temperature and relative humidity as the inputs, as detailed in our previous publications (Xu et al., 2020, 2022b, 2023). The model output results based on our data set showed that 94 % and 90 % of NO_3^- were in the aerosol phase in the cold and warm periods, respectively. Hence, the predictions of pH and ALW were conducted without considering gaseous nitric acid (Guo et al., 2015; Wang et al., 2021b). A total of 78 % and 21 % of NH_4^+ was in the aerosol phase in the cold and warm periods, respectively. Moreover, it is important to note that gaseous NH_3 measurements were not conducted and ammonia partitioning was not considered in this study. Thus, a bias correction of 1 pH unit was applied to calculate the aerosol pH values (Guo et al., 2015; Wang et al., 2021). The concentrations of ambient $\cdot\text{OH}$ were predicted using empirical formula (Ehhalt and Rohrer, 2000; Wang et al., 2020).

3 Results and discussion

3.1 Overall molecular characterization of organic aerosols

Figure 1a and c show the mass spectra of organic compounds detected in ESI+ and ESI-, respectively. More compounds were identified in ESI+ (1885 molecular formulas) than in ESI- (1091 molecular formulas) (Table S2), which was similar to previous reports about the molecular characteristic of biomass burning aerosols and urban aerosols (Jiang et al., 2022; Y. Wang et al., 2017). The molecular weights of the compounds with relatively high signal intensity mainly ranged from 100 to 500 Da in ESI+, which was larger than those (100–300 Da) observed in the urban (Changchun, Guangzhou, and Shanghai) (K. Wang et al., 2021) and agricultural (Suixi) (Y. Wang et al., 2017) regions of China. In contrast, the species with the strong signal intensity fell between 100 and 300 Da in ESI-. This mass range detected in Ürümqi organic aerosols was comparable to previous observations in urban (Xi'an) aerosols (Han et al., 2023) but significantly lower than that in firework-related urban (Beijing) aerosols (300–400 Da) (Xie et al., 2020). On average, the molecular number and relative abundance of CHON compounds (150–500 Da) were dominant in ESI+, accounting for 45.57 % of the total molecular number and 62.70 ± 6.83 % of the total signal intensity (Fig. 1a and Table S2). CHO compounds was the second-most abundant category (28.76 ± 4.75 % of the total signal intensity), followed by CHN compounds. However, previous observations conducted in Shanghai, Guangzhou, and Changchun

suggested that the compounds in ESI+ were dominated by CHN and CHON species (K. Wang et al., 2021). In ESI-, although the number of CHON compounds was less than CHO, the relative abundance of CHON compounds (150–250 Da) was higher (Fig. 1d and Table S2). The finding was consistent with the results obtained in Shanghai and Changchun but different from the case in Guangzhou (K. Wang et al., 2021). The average H/C ratios of CHO (1.62–1.66) and CHON (1.79–1.83) compounds in ESI+ mode (Table S3) were higher than those (0.94–1.13 for CHO and 1.27–1.47 for CHON) in Changchun, Shanghai, and Guangzhou (K. Wang et al., 2021). However, the average O/C ratios of CHO (0.25–0.3) and CHON (0.22–0.3) compounds in ESI+ mode (Table S3) were less than those (0.42–0.43 for CHO and 0.27–0.45 for CHON) in the urban areas (Shanghai and Guangzhou) (K. Wang et al., 2021). Overall, these dissimilarities in molecular characteristics of organic aerosols between Ürümqi and other areas may be attributed to their different sources and formation mechanisms.

Figure 1b and d show the time series of the fractional distributions of various organic matter categories in different ion modes. The abundance of CHO compounds in ESI+ exhibited a temporal variation similar to that of CHON compounds ($r = 0.51$, $P < 0.01$), with increased levels in the warm period. This indicated that CHO compounds may be important precursors for the formation of NOCs (via reactions in the gas- and/or particle-phases) or that they have similar origins. Previous simulation experiments have demonstrated that higher temperatures increase the concentration of oxygenated organic molecules, while lower temperatures can allow less oxidized species to condense (Stolzenburg et al., 2018; Frege et al., 2018). In addition, solar radiation and atmospheric oxidation capacity are also important factors promoting the formation of more oxygenated organic molecules (Li et al., 2022; Liu et al., 2022). Air temperature, radiation, and atmospheric oxidation capacity were much higher in the warm period than in the cold period in Ürümqi (Table S1) (Wan et al., 2021), which may be partly responsible for increased abundances of CHO and CHON compounds in the warm period. However, the abundance of CHN compounds tended to increase from the warm period to the cold period. Since the ESI+ mode is highly sensitive to protonatable species, organic amines were expected to predominate the CHN compounds (Han et al., 2023; K. Wang et al., 2021). It is well documented that the formation of amine salt in the particle phase is tightly associated with aerosol acidity and water (Liu et al., 2023). Thus, the reduced pH value and increased ALW level in the cold period (Table S1) provided greater potential for converting gaseous amines into particles.

In ESI- mode, the abundances of CHON and CHO compounds exhibited a significantly increased level in the cold period (Fig. 1d), a variation pattern which was completely opposite to the case in ESI+ mode. The ESI- mode is more sensitive to deprotonatable compounds like nitrophenols, organic nitrates, organosulfates, and organic acids (Jiang et al.,

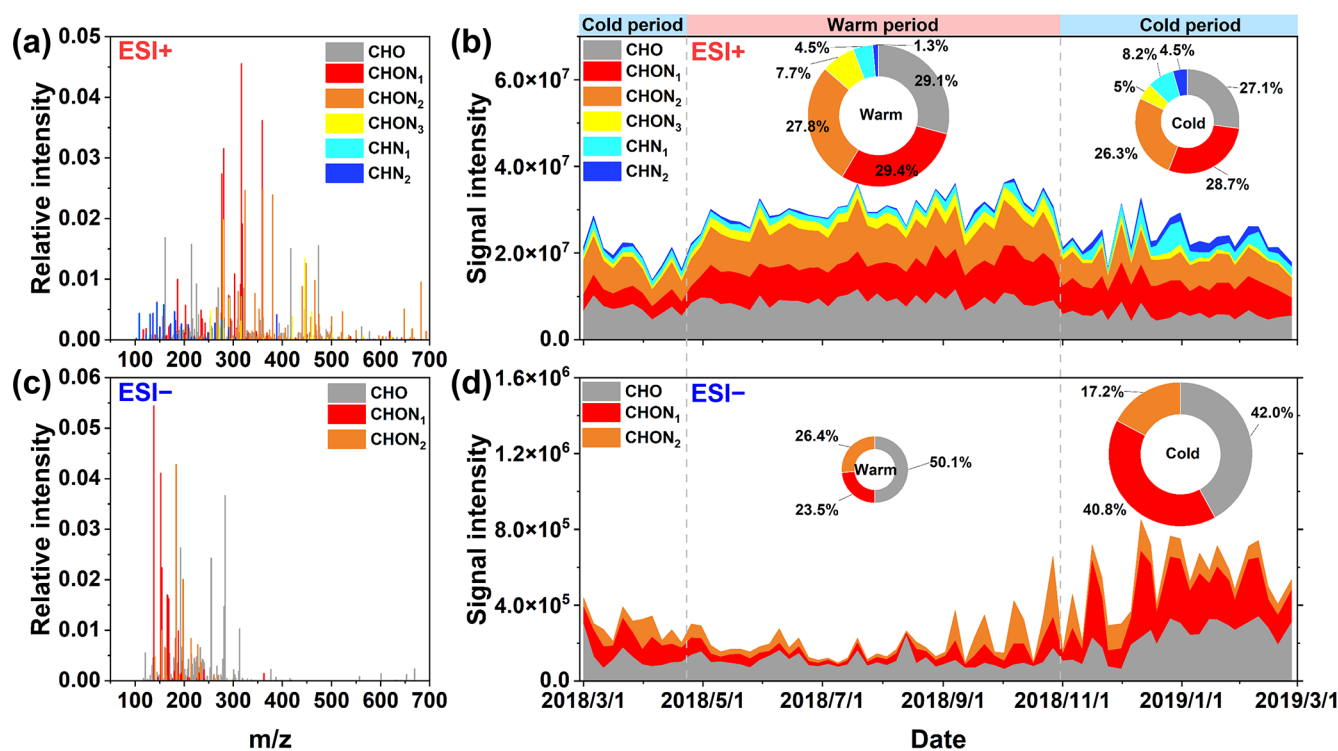


Figure 1. The reconstructed mass spectrum distribution of the detected species in PM_{2.5} in (a) ESI+ and (c) ESI– modes during the whole campaign. Temporal variations in the fractional distribution of classified compounds in (b) ESI+ and (d) ESI– modes. The ring diagrams inside (b) and (d) show the signal intensity fractions of classified compounds, the size of which is proportional to the total signal intensity of all species detected in PM_{2.5} in different periods.

2022; Lin et al., 2012). The formations of these compounds were highly impacted by ALW and aerosol acidity (Ma et al., 2021; Smith et al., 2014; Zhou et al., 2023; Xu et al., 2023). However, Ürümqi has dry and dusty weather, particularly in warm period, resulting in a quite low ALW concentration ($1.86 \pm 1.90 \mu\text{g m}^{-3}$) in the warm period (Table S1). Moreover, the calculated mean pH value was 6.86 ± 1.71 (Table S1) during the warm period, which implies that the fine aerosol particles in the warm period in Ürümqi was neutral or slightly alkaline. Obviously, the aerosol characteristics of the warm period in Ürümqi may hinder the formation of these organic compounds measured in ESI– mode. In contrast, the increased ALW concentration and decreased pH value during the cold period can facilitate the formation of CHO and CHON compounds through the partitioning of gas-phase species to the particles and subsequent aqueous phase reactions (Xu et al., 2020, 2023). Furthermore, the total signal intensity of CHO compounds was significantly correlated with that of CHON ($r = 0.62$, $P < 0.01$), indicating that they may have similar origins or that CHO compounds may serve as important precursors for CHON compound formation. In general, the differentiated seasonal variation patterns for the different types of NOCs measured here can be attributed to the unique meteorological conditions in Ürümqi and different ionization mechanisms in ESI+ and ESI– modes. The

sources and formation mechanisms of NOCs will be further discussed in the following sections.

3.2 Seasonally differential sources and formation mechanisms of CHON compounds

CHON compounds can be derived from the reactions between CHO species and reactive nitrogen species (NO_x , NH_3 , and NH_4^+) (Lee et al., 2016; De Haan et al., 2017), as also partly implied by significant positive correlations ($r = 0.51$ – 0.62 , $P < 0.01$) between total signal intensity of CHO and CHON compounds in both ESI+ and ESI– modes. Thus, CHO compounds were further classified based on their OS_C values to preliminarily explore their origins and linkages with CHON compound formation (Fig. 2a and b). In ESI+ mode, the OS_C values of the detected CHO compounds (-1.75 to 0.5) were higher than those of primary vehicle exhausts (-2.0 to -1.9) (Aiken et al., 2008), likely indicating a weak (or indirect) contribution of primary vehicle exhausts to CHO molecules in Ürümqi. The signal intensity of BBOA dominated the total OA signal intensity and was higher in the warm period than in the cold period (Fig. 2e). However, previous studies conducted in China (e.g., Beijing, Xi'an, Shanghai, and Liaocheng) suggested that biomass burning was more significant in the cold sea-

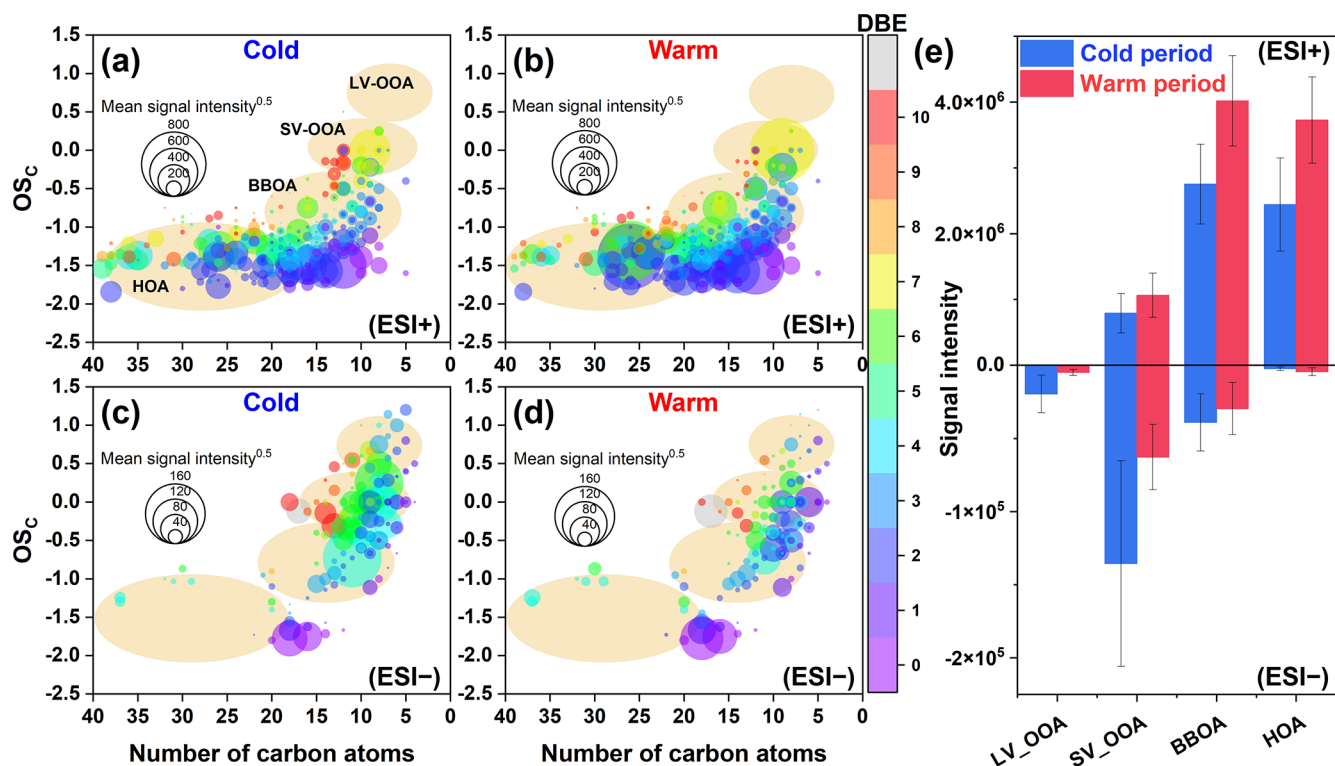


Figure 2. OSC values of CHO molecules detected in (a, b) ESI+ and (c, d) ESI– modes in PM_{2.5} collected from different periods (cold vs. warm). The size and color of the circle indicate the mean signal intensity and DBE value of compounds, respectively. The light orange background indicates the areas of LV-OOA, SV-OOA, BBOA, and HOA (Kroll et al., 2011), according to which (e) the mean signal intensity of classified compounds was calculated for samples from different periods.

sons (Li et al., 2023; X. Wang et al., 2017; Chen et al., 2017; Wang et al., 2009, 2018; Zhang et al., 2022). Furthermore, we found that the oxygen-poor unsaturated aliphatic compounds showed a high signal intensity in the warm period and that the signal intensities of all categories of compounds in the warm period were weakly correlated with atmospheric oxidants (i.e., O₃ and •OH) ($r < 0.1$, $P > 0.05$). Thus, the formation or source of CHO compounds in the warm period may not be mainly controlled by high atmospheric oxidation but rather by biomass burning, which was distinguished from previous reports (Duan et al., 2020; Kondo et al., 2007; Zhang et al., 2023). This consideration was also supported by the fact that there were significantly more fire spots in the warm period than in the cold period (Fig. 3). It should be noted that the materials used for biomass burning in the cold period in rural China are typically aged plant tissues, such as dead branches of pine trees, dead branches of shrubs, corn straw, and rice straw (Fig. S3), while biomass burning in the warm season is mainly attributed to forest fires or wildfires (relatively fresh biomass). Accordingly, a large number of fresh biomass material burning occurred from April to October each year in neighboring countries (e.g., Kazakhstan) (Xu et al., 2021) or the region of Ürümqi (due to drought)

(Fig. 3) may be largely responsible for high CHO compound abundance in the warm period.

The CHO species in ESI– had higher OSC (−1.85 to 0.1) than those in ESI+ (−1.85 to 0.25) (Fig. 2c and d), which was consistent with a recent study conducted in Guangzhou, China (Zou et al., 2023). The predominant subgroups of CHO in ESI– were BBOA (66.4 % of total signal intensity) and SV-OOA (23.1 % of total signal intensity), which was different from the observation in Shanghai (dominated by SV-OOA and LV-OOA) (X. Wang et al., 2017). Additionally, some specific saturated and unsaturated aliphatic CHO substances (i.e., C_{12–18}H_nO₂) in ESI– showed higher abundance in the warm season than in the cold season, which was contrary to the variation pattern of other CHO compounds. These C_{12–18}H_nO₂ compounds were found to be mainly fatty acids, such as stearic acid (C₁₈H₃₆O₂), oleic acid (C₁₈H₃₄O₂), linoleic acid (C₁₈H₃₂O₂), palmitic acid (C₁₆H₃₂O₂), and palmitoleic acid (C₁₆H₃₀O₂) (Fig. S4), all of which usually accumulate in plants, particularly *Suaeda aralocaspica* (Hogg and Gillan, 1984; Wang et al., 2011). Interestingly, this plant was widely distributed in central Asia, as well as on the southern edge of the Junggar Basin in Xinjiang, China (Wang et al., 2011). Although fatty acids can also originate from food cooking (Zhao et al., 2007),

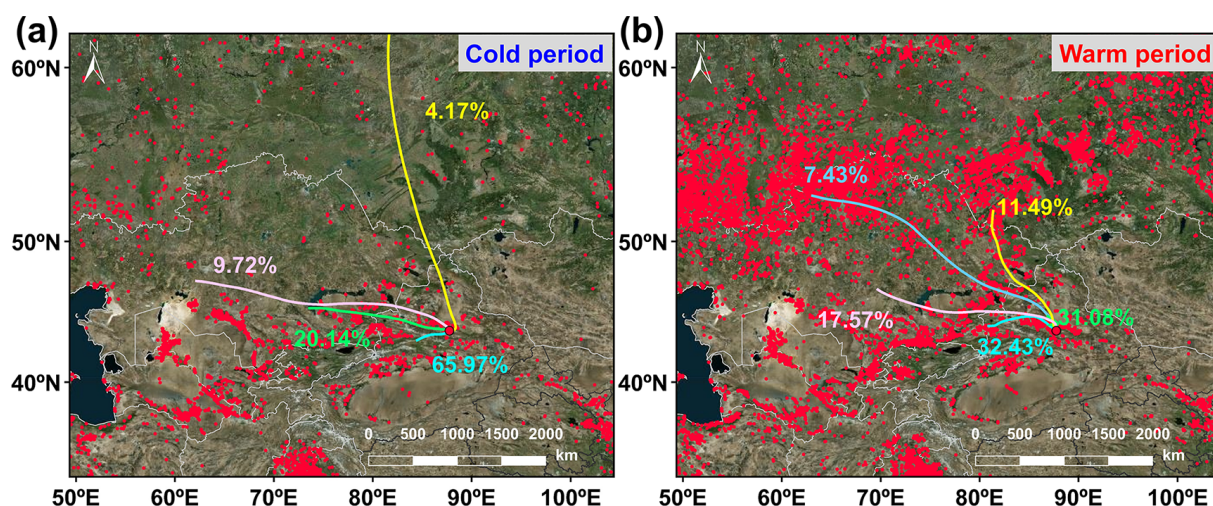


Figure 3. The 3 d (72 h) back trajectories illustrating the typical air mass flows to the study site during the (a) warm and (b) cool periods. Fire spots are shown in red, based on NASA active fire data (VIIRS 375 m, https://firms.modaps.eosdis.nasa.gov/active_fire/, last access: 11 October 2023). The map is derived from © MeteInfoMap (version 3.6.2) (Chinese Academy of Meteorological Sciences, China).

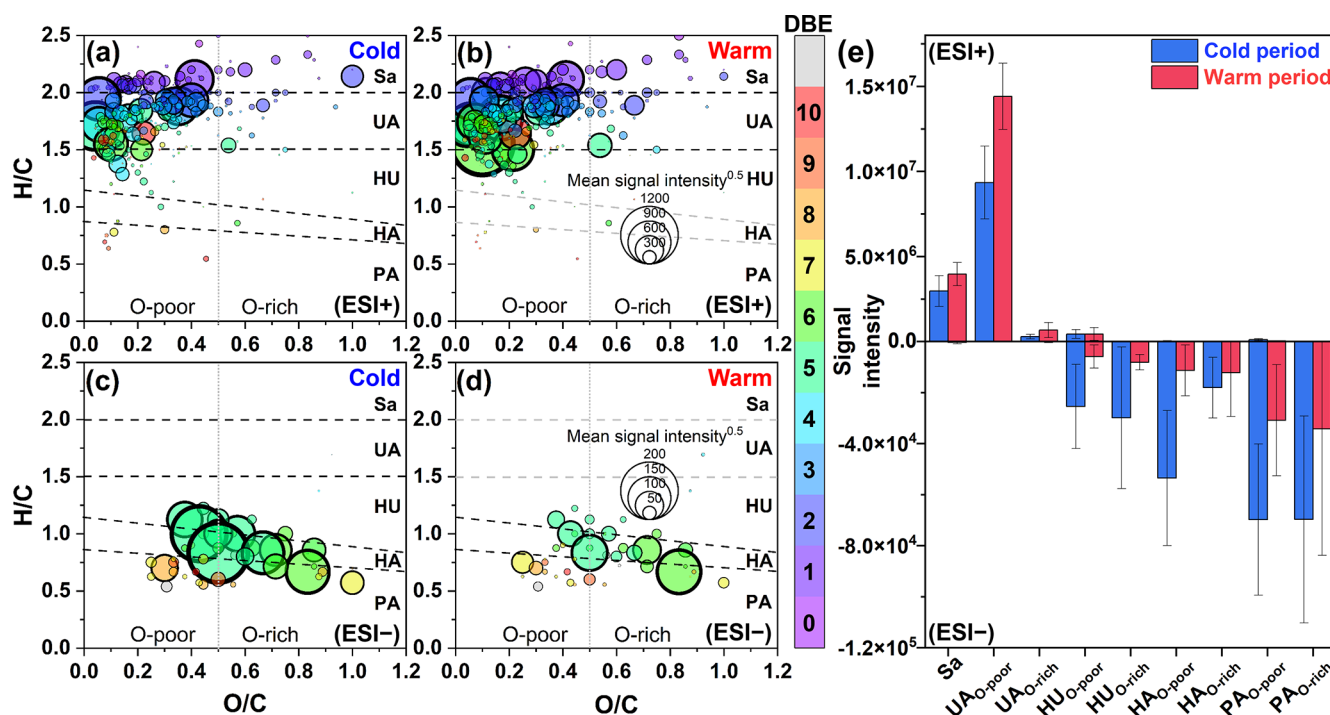


Figure 4. Van Krevelen diagrams of CHON molecules detected in (a, b) ESI+ and (c, d) ESI– modes in PM_{2.5} collected from different periods (cold vs. warm). The subgroups in the panels include saturated-like (Sa), unsaturated aliphatic-like (UA), highly unsaturated-like (HU), highly aromatic-like (HA), and polycyclic aromatic-like (PA) compounds, further distinguishing between oxygen-poor and oxygen-rich compounds with an oxygen-to-carbon ratio of 0.5. The size and color of the circle indicate the mean signal intensity and DBE value of compounds, respectively. The (e) mean signal intensity of classified compounds was calculated for samples from different periods.

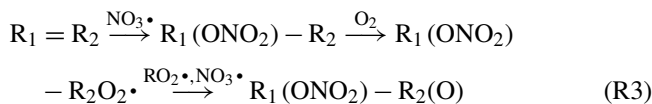
there seem to be no seasonal differences in cooking behavior locally. Thus, these results further confirmed our consideration that the abundance of CHO compounds in the warm period was highly impacted by fresh biomass material burning (e.g., forest fires or wildfires).

CHON molecules in ESI+ were mainly identified as unsaturated aliphatic-like compounds that are oxygen poor (Fig. 4a and b), accounting for more than 70 % of the total signal intensities of CHON species (Fig. S5). The signal intensity of CHON species in ESI+ was greater in the warm

period than in the cold period (Fig. 4e). Moreover, BBOA contributed to 56.9 % of the total CHON signal intensity in the warm period (Fig. S6). These characteristics of CHON compounds were similar to those of CHO. Considering a significant positive correlation ($r = 0.62$, $P < 0.01$) between the total signal intensity of CHO and CHON compounds in ESI+, we thus concluded that primary sources (i.e., fresh biomass material burning) were also one of the main sources of CHON compounds. In this study, CHON compounds with O/N < 3 contributed 76.48 ± 1.11 % of total CHON species in ESI+ (Fig. S7), which was much larger than the results observed in urban Tianjin in winter (less than 20 %) (Zhong et al., 2023). In particular, C₁₆H₃₃ON, C₁₈H₃₇ON, C₁₈H₃₅ON, C₁₈H₃₃ON, C₁₈H₃₁ON, and C₂₀H₃₃ON showed a high abundance, together accounting for 55.04 ± 7.09 % of the total CHON abundance (Table S4). The carbon number of these compounds was consistent with that of fatty acids mentioned above; moreover, their abundances showed a positive correlation ($r = 0.43$ – 0.81 , $P < 0.01$) with the abundances of corresponding fatty acids in the warm period. In contrast, these CHON compounds only showed a weak correlation ($r = -0.24$ – 0.33) with atmospheric oxidants (e.g., •OH, O₃, and NO_x). Thus, the formation mechanism of biomass-burning-related NOCs in Ürümqi during the warm period may be the interaction between fatty acids and reduced nitrogen species (e.g., NH₃) rather than the oxidation pathway involving CHO compounds and NO_x.

A recent laboratory study has suggested that NH₃ produced during the thermal degradation of amino acids can react with oleic acid from the pyrolysis of triglycerides to form amides (Reaction R1) (Ditto et al., 2022a). As discussed above, the combustion of fresh biomass materials (e.g., forest fires or wildfires) can release abundant fatty acids. In addition, wildfires can also emit large amounts of NH₃, with an average emission factor more than twice the NH₃ emission factor of agricultural fires (Tomsche et al., 2023). According to tandem mass spectrometry (MS/MS) analysis (Table S5), potential fatty-acid-derived NOCs were indeed identified as amides. Thus, we proposed that the high temperature generated during wildfires or forest fires provides suitable conditions for the reaction of carboxylic acids and NH₃ to form amides. The specific process was presented in Fig. 5 (Pathway 1). It has been suggested that atmospheric oxidants can oxidize olefins (Reactions R2 and R3) to form hydroxyl nitrates and carbonyl nitrates (Perring et al., 2013). Therefore, fatty acids (oleic acid as a representative) released from fresh biomass material burning may also rely on oxidation pathways to form NOCs (Fig. 5, Pathway 2). It is worth noting that some products with double bonds after the amidation of unsaturated fatty acids can continue to undergo Reactions (R2) and (R3) in the atmosphere, resulting in the formation of nitrooxy amides (Fig. 5, Pathway 3). However, we found that the abundance of oleic-acid-derived amides via Pathway 1 in the warm period was more than 100 times higher than that of NOCs with –ONH₂ (thus, the

impact of ionization efficiency is expected to be less than 100 times) from Pathways 3. In the cold period, the abundance of fatty-acids-derived amides decreased dramatically (Figs. 5 and S8). Thus, the overall results demonstrated that the combustion of fresh biomass materials indeed contributed significantly to aerosol NOCs (e.g., amides) in the warm period in Ürümqi.



The CHON species detected in ESI– were mainly aromatic-like compounds, whose signal intensities were significantly greater in the cold period than in the warm period (Figs. 4c, e and S5). Moreover, we found that several nitro-aromatic compounds, including C₆H₅O₃N, C₆H₅O₄N, C₇H₇O₃N, C₇H₇O₄N, C₇H₅O₅N, and C₈H₉O₃N (confirmed by their authentic standards in the LC/MS analysis), contributed up to 50 % of the total CHON (ESI– mode) intensity (Table S6). Other NOCs with relatively high signal intensity were mainly O_{4–6}N₂ species (contributed up to 25 %), such as C₆H₄O₅N₂, C₇H₄O₇N₂, C₇H₆O₅N₂, and C₇H₆O₆N₂, which have been suggested to be associated with secondary photochemical or multiphase chemical processes (Harrison et al., 2005; Cecinato et al., 2005; Salvador et al., 2021). However, the abovementioned nitro-aromatic compounds, including C₆H₅O₃N (nitrophenol), C₆H₅O₄N (nitrocatechol), C₇H₇O₃N (methyl-nitrophenol), and C₇H₇O₄N (methyl-nitrocatechol), were primarily identified as tracers of straw and wood burning (aged biomass materials commonly used in suburban and rural China) (Iinuma et al., 2010; Kourtchev et al., 2016). A study about molecular characterization (ESI– mode) of water-soluble aerosols emitted from the combustion of aged biomass materials (i.e., dry corn straw, rice straw, and pine branches) and coal showed that OA from aged biomass burning typically contained much more nitro compounds and/or organonitrates than that from coal, while OA from coal smoke contained more sulfur-containing compounds (Song et al., 2018). Thus, the aged biomass burning associated with winter heating rather than coal combustion may contribute a significant amount of aerosol NOCs (e.g., nitrophenols) in wintertime Ürümqi. However, it does not necessarily suggest that the importance of multiphase chemistry in the formation of NOCs was ignorable, as indicated by relatively high signal intensity of O_{4–6}N₂ species. In general, the differential molecular characteristics of CHON species in different seasons in Ürümqi can largely be attributed to different impacts of the combustion of fresh and aged biomass materials.

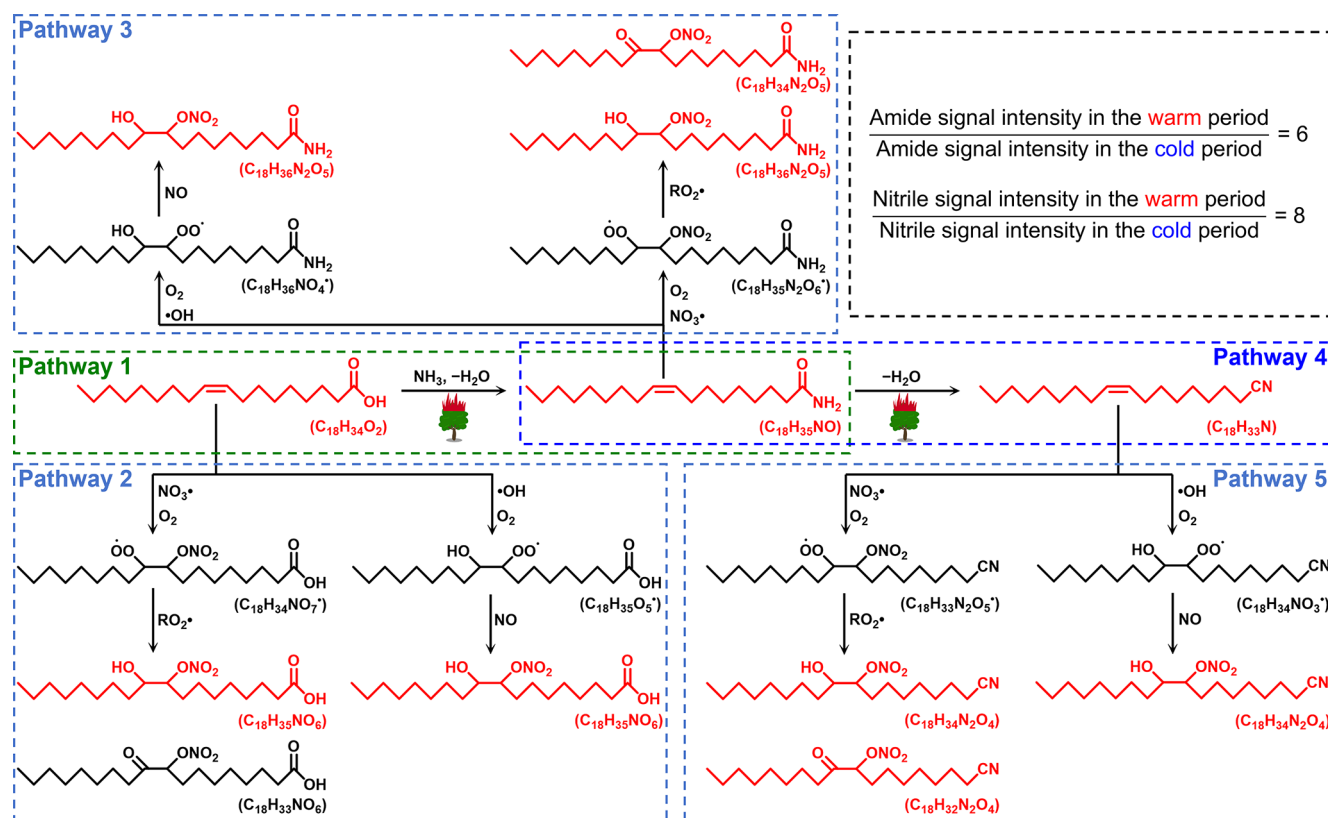


Figure 5. Proposed pathways for the reactions of carboxylic acids (oleic acid as a representative) with reactive nitrogen and atmospheric oxides to form the observed NOCs in PM_{2.5} under the influence of the high temperature generated during wildfires or forest fires. Compounds observed in PM_{2.5} were shown in red.

3.3 CHN molecule evidence of fresh and aged biomass burning in different periods

Figure 6a and b present the van Krevelen diagram of CHN compounds in the cold and warm periods. The CHN₁ compounds with relatively high signal intensity mainly contained 7–20 carbon atoms, among which C₅H₅N(CH₂)_n, C₉H₇N(CH₂)_n, and C₁₃H₉N(CH₂)_n were dominant (78.68 ± 7.59 % of the total signal intensity of CHN₁ compounds in the cold period, Table S7). C₅H₅N(CH₂)_n could be identified as pyridine and its homologues, which have been detected in freshly discharged BBOA (Dou et al., 2015). Additionally, the abundance of C₅H₅N(CH₂)_n was positively correlated with that of C₉H₇N(CH₂)_n, C₁₃H₉N(CH₂)_n, and nitro-aromatic compounds mentioned above ($r = 0.46$ – 0.81 , $P < 0.01$), particularly in the cold period with aged biomass burning for heating. We further found that both the total signal intensity and aromaticity of CHN₁ species were much higher in the cold period (AI_{mod} of 0.52) than in the warm period (AI_{mod} of 0.35) (Figs. 6 and S9). It has been suggested that aged leaves contain more aromatic compounds compared to fresh leaves (Jian et al., 2016). Thus, the overall results implied that aged biomass burning had an important contribution to the variation of CHN₁ compounds. In particu-

lar, the intensity of CHN₁ compounds was significantly negatively correlated with the concentration of O₃ and •OH ($r = -0.44$ – 0.53 , $P < 0.01$), suggesting that atmospheric oxidation processes were the potential pathway for amine removal rather than the sources of particle amine salts (Zahardis et al., 2008; Qiu and Zhang, 2013). This result differed from the previous case, which showed that the formation processes of CHN₁ and its homologs in Guangzhou (South China) were tightly related to photo-oxidation processes (Jiang et al., 2022). The CHN₂ species showed a similar temporal variation pattern to the CHN₁ species. Moreover, the abundances of total CHN₂ and major components (C_{8–11}H₈N₂(CH₂)_n, C₁₀H₁₄N₂(CH₂)_n, C₁₀H₁₆N₂(CH₂)_n, and C₅H₈N₂(CH₂)_n) were positively correlated with that of total CHN₁ ($r = 0.55$ – 0.90 , $P < 0.01$) but negatively correlated with the concentration of O₃ and •OH ($r = -0.43$ – 0.60 , $P < 0.01$). Clearly, aged biomass burning, particularly in the cold period, also exerted significant impacts on the abundance of CHN₂ compounds, which was also supported by several previous studies (Laskin et al., 2009; Y. Wang et al., 2017; Song et al., 2022). A study about molecular characterization (ESI+ mode) of humic-like substances emitted from the combustion of aged biomass materials (i.e., dry corn straw, rice straw, and pine branches) and coals showed that OA from

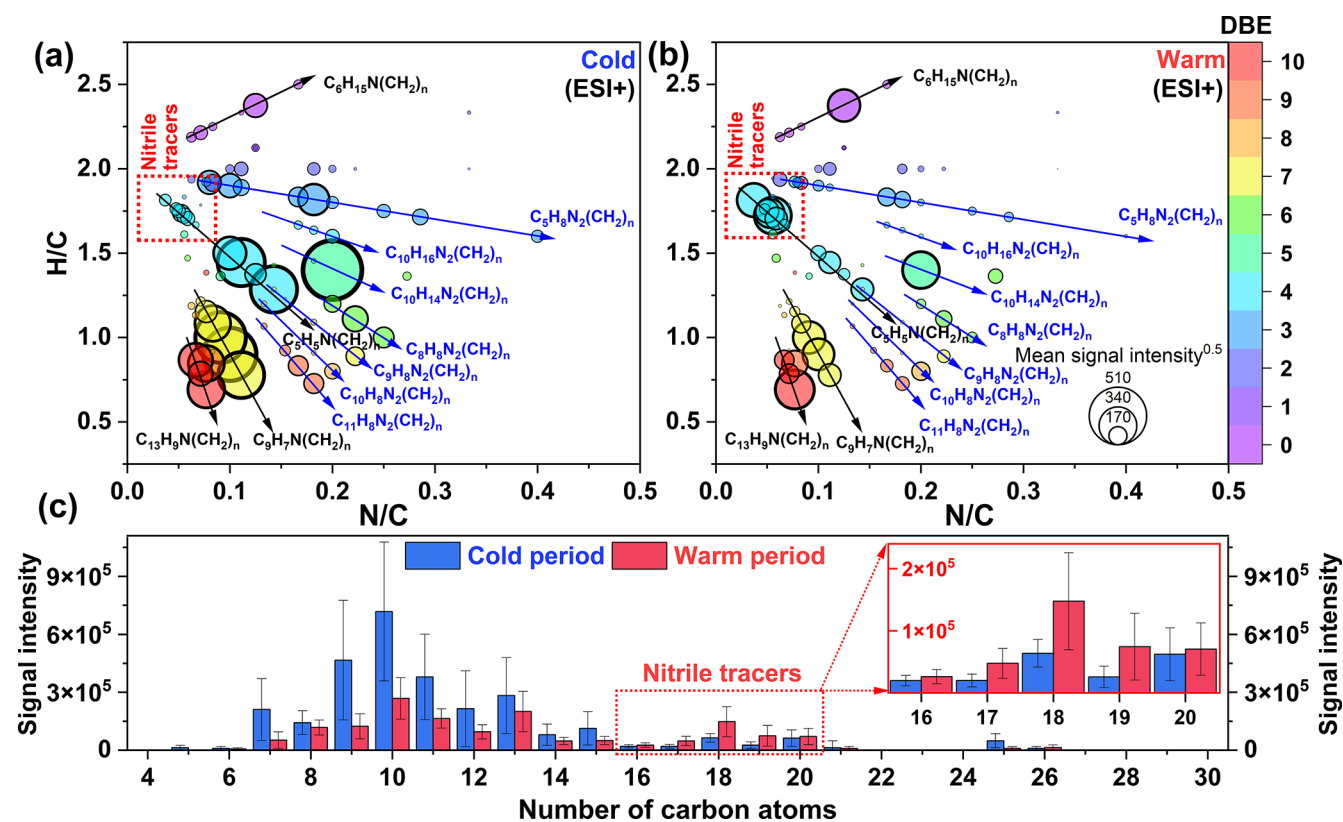


Figure 6. Van Krevelen diagrams of CHN molecules detected in PM_{2.5} collected from the (a) cold and (b) warm periods. The size and color of the circle indicate the mean signal intensity and DBE value of compounds, respectively. The mean signal intensity distributions of (c) carbon atoms in CHN molecules detected in PM_{2.5} collected from the cold and warm periods.

aged biomass burning typically contained much more CHN₂ compounds (55 %–64 %) than that from coal (20 %–37 %), while OA from coal smoke showed more CHN₁ compounds (78 %–84 %) compared to that from aged biomass materials (15 %–22 %) (Song et al., 2022). In this study, the signal intensity of CHN₁ compounds in the cold period was about 40 % higher than that in the warm period, while that of CHN₂ compounds showed a 160 % increase from the warm period to the cold period. Thus, although the contribution of fossil fuel (e.g., coal) combustion to NOCs in the cold period cannot be ignored, our results at least suggested that the biomass-burning-derived CHN compounds showed a more significant increase compared to coal combustion-derived compounds from the warm period to the cold period in Ürümqi.

Interestingly, we found some CHN species with 16–20 carbon atoms showed higher abundance in the warm period than in the cold period, a pattern opposite to that of all other CNH compounds (Fig. 6c). These C_{16–20}N₁H_x compounds were further identified as alkyl nitriles (Table S5) (Simoneit et al., 2003). In addition, the carbon number of the identified alkyl nitriles was consistent with those of amides previously proposed to be produced by fresh biomass burning. Thus, we proposed that fresh biomass material burning in

the warm period may provide a continuous high-temperature environment to promote the dehydration of amides (Fig. 5, Pathway 4). These alkyl nitriles with double bonds can continue to undergo Reactions (R2) and (R3) (Fig. 5, Pathway 5). However, the signal intensity of the nitrooxy products in the warm period was insignificantly correlated with the concentration of O₃, •OH, and NO_x ($P > 0.05$), likely indicating a weak influence of atmospheric oxidation on alkyl nitrile removal in this site. The high-temperature dehydration of amides (e.g., erucamide) to form alkyl nitriles (e.g., erucyl nitrile) has been demonstrated by Simoneit et al. (2003) in a laboratory simulation experiment. A study on BBOA also showed that alkyl nitriles can serve as indicators of biomass burning in the ambient atmosphere (Radzi Bin Abas et al., 2004). Furthermore, the abundance of identified alkyl nitriles initially increased from March and peaked in September and October (Fig. S10), a pattern which was consistent with the interannual variation in wildfire areas (more in the warm period) in Central Asian countries (Xu et al., 2021). Although cooking is also a potential source of alkyl nitriles (Schauer et al., 1999), this activity does not have seasonal differences. In contrast, the dramatically increased abundance of aromatic CNH compounds in the cold period (Fig. S9) can be attributed to the aqueous reactions of

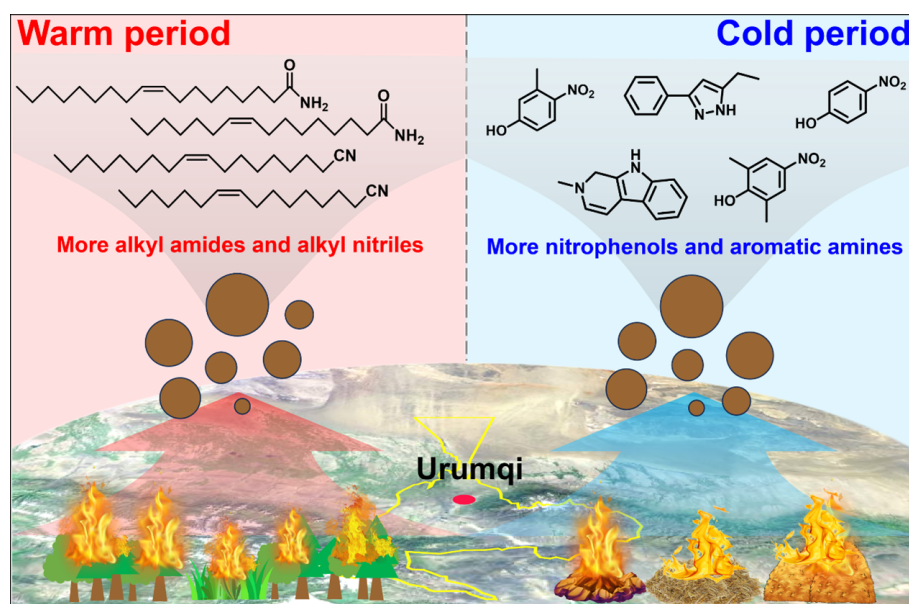


Figure 7. Conceptual picture showing the differential impacts of combustion of fresh and aged biomass materials on aerosol NOCs in suburban Ürümqi. The map was derived from © Baidu Maps (BIDU, China).

amines emitted from aged biomass material and coal combustion with acidic substances, as indicated by significant correlations ($r = 0.61\text{--}0.95$, $P < 0.01$) between total CHN abundance and SO_4^{2-} and NO_3^- concentrations. These findings further confirmed that the NOCs from the combustion of fresh biomass materials in the warm period in suburban Ürümqi were compositionally different from those from aged biomass burning in the cold period.

4 Conclusions

The complexity of NOCs restricts our understanding of its sources and formation processes. In this study, the molecular compositions of organic aerosols in PM_{2.5} collected in Ürümqi over a one-year period were systematically characterized in both ESI⁻ and ESI⁺ modes, with a major focus on NOCs. A large amount of NOCs were identified, showing that NOCs in relatively highly oxidative and reduced forms can be roughly distinguished via these two ionization modes. Based on the identification of molecular markers of amides and alkyl nitriles (much higher in the warm period) and the analysis of their formation mechanisms (less contribution of atmospheric oxidation), we highlighted the important contribution of combustion of fresh biomass materials such as forest fires and wildfires to NOCs in the warm season in Ürümqi. In contrast, the dramatically increased abundances of aromatic CNH compounds and nitro-aromatic CHON compounds (mainly nitrophenols) in the cold period were tightly associated with the impacts of aged biomass material burning. These results were illustrated in a diagram (Fig. 7).

Biomass materials in rural China were typically aged plant tissues, as mentioned above. Fresh biomass materials (e.g., green vegetation) with the enrichment of oils and proteins can exist in forest fires or wildfires. Indeed, previous studies have suggested that biomass burning can lead to the formation of aerosol amines and nitriles. However, field observation studies have yet to pay attention to the differences in aerosol NOCs emitted from the combustion of fresh and aged biomass materials. For the first time, our results reveal that fresh biomass material combustion can contribute more amines and nitriles than aged biomass material combustion. Generally, this study provides field evidence on the differential impacts of the combustion of fresh and aged biomass materials on aerosol NOCs, improving our current understanding of the molecular compositions of organic nitrogen aerosols in a vast territory with a sparse population in north-western China. Moreover, according to the fact that the studied site is highly affected by combustion emissions of different types of biomass materials, future work is needed to deeply understand the quantitative contributions of different types of biomass burning to OA in China.

Data availability. The data in this study are available at <https://doi.org/10.5281/zenodo.10453929> (Ma et al., 2024).

Supplement. Details of chemical analysis and data processing, 8 tables (Tables S1–S8), and 10 extensive figures (Figs. S1–S10) are provided in the Supplement. The supplement related to this article is available online at: <https://doi.org/10.5194/acp-24-4331-2024-supplement>.

Author contributions. YX designed the study. YJM, TY, and HWX performed field measurements and sample collection. YJM and TY performed chemical analysis. YX and YJM performed data analysis. YX and YJM wrote the original manuscript. YX, YJM, HWX, and HYX reviewed and edited the manuscript.

Competing interests. The contact author has declared that none of the authors has any competing interests.

Disclaimer. Publisher's note: Copernicus Publications remains neutral with regard to jurisdictional claims made in the text, published maps, institutional affiliations, or any other geographical representation in this paper. While Copernicus Publications makes every effort to include appropriate place names, the final responsibility lies with the authors.

Acknowledgements. The authors are very grateful to the editor and the anonymous referees for the kind and valuable comments that improved the paper.

Financial support. This research has been supported by the National Natural Science Foundation of China (grant no. 42303081) and the Science and Technology Innovation Plan Of Shanghai Science and Technology Commission (grant no. 22YF1418700).

Review statement. This paper was edited by Eleanor Browne and reviewed by two anonymous referees.

References

- Aiken, A. C., Decarlo, P. F., Kroll, J. H., Worsnop, D. R., Huffman, J. A., Docherty, K. S., Ulbrich, I. M., Mohr, C., Kimmel, J. R., Sueper, D., Sun, Y., Zhang, Q., Trimborn, A., Northway, M., Ziemann, P. J., Canagaratna, M. R., Onasch, T. B., Alfarra, M. R., Prevot, A. S., Dommen, J., Duplissy, J., Metzger, A., Baltensperger, U., and Jimenez, J. L.: O/C and OM/OC ratios of primary, secondary, and ambient organic aerosols with high-resolution time-of-flight aerosol mass spectrometry, *Environ. Sci. Technol.*, 42, 4478–4485, <https://doi.org/10.1021/es703009q>, 2008.
- Altieri, K. E., Fawcett, S. E., Peters, A. J., Sigman, D. M., and Hastings, M. G.: Marine biogenic source of atmospheric organic nitrogen in the subtropical North Atlantic, *P. Natl. Acad. Sci. USA*, 113, 925–930, <https://doi.org/10.1073/pnas.1516847113>, 2016.
- Bandowe, B. A. M. and Meusel, H.: Nitroated polycyclic aromatic hydrocarbons (nitro-PAHs) in the environment – A review, *Sci. Total Environ.*, 581–582, 237–257, <https://doi.org/10.1016/j.scitotenv.2016.12.115>, 2017.
- Bátori, Z., Erdős, L., Kelemen, A., Deák, B., Valkó, O., Gallé, R., Bragina, T. M., Kiss, P. J., Kröel-Dulay, G., and Tölgyesi, C.: Diversity patterns in sandy forest-steppes: a comparative study from the western and central Palaearctic, *Biodivers. Conserv.*, 27, 1011–1030, <https://doi.org/10.1007/s10531-017-1477-7>, 2018.
- Cape, J. N., Cornell, S. E., Jickells, T. D., and Nemitz, E.: Organic nitrogen in the atmosphere – Where does it come from? A review of sources and methods, *Atmos. Res.*, 102, 30–48, <https://doi.org/10.1016/j.atmosres.2011.07.009>, 2011.
- Cecinato, A., Di Palo, V., Pomata, D., Tomasi Scianò, M. C., and Possanzini, M.: Measurement of phase-distributed nitrophenols in Rome ambient air, *Chemosphere*, 59, 679–683, <https://doi.org/10.1016/j.chemosphere.2004.10.045>, 2005.
- Chen, J., Li, C., Ristovski, Z., Milic, A., Gu, Y., Islam, M. S., Wang, S., Hao, J., Zhang, H., He, C., Guo, H., Fu, H., Miljevic, B., Morawska, L., Thai, P., Lam, Y. F., Pereira, G., Ding, A., Huang, X., and Dumka, U. C.: A review of biomass burning: Emissions and impacts on air quality, health and climate in China, *Sci. Total Environ.*, 579, 1000–1034, <https://doi.org/10.1016/j.scitotenv.2016.11.025>, 2017.
- De Haan, D. O., Hawkins, L. N., Welsh, H. G., Pednekar, R., Casar, J. R., Pennington, E. A., de Loera, A., Jimenez, N. G., Symons, M. A., Zauscher, M., Pajunoja, A., Caponi, L., Cazau-nau, M., Formenti, P., Gratien, A., Pangui, E., and Doussin, J.-F.: Brown Carbon Production in Ammonium- or Amine-Containing Aerosol Particles by Reactive Uptake of Methylglyoxal and Photolytic Cloud Cycling, *Environ. Sci. Technol.*, 51, 7458–7466, <https://doi.org/10.1021/acs.est.7b00159>, 2017.
- Ditto, J. C., Abbatt, J. P. D., and Chan, A. W. H.: Gas- and Particle-Phase Amide Emissions from Cooking: Mechanisms and Air Quality Impacts, *Environ. Sci. Technol.*, 56, 7741–7750, <https://doi.org/10.1021/acs.est.2c01409>, 2022a.
- Ditto, J. C., Machesky, J., and Gentner, D. R.: Analysis of reduced and oxidized nitrogen-containing organic compounds at a coastal site in summer and winter, *Atmos. Chem. Phys.*, 22, 3045–3065, <https://doi.org/10.5194/acp-22-3045-2022>, 2022b.
- Ditto, J. C., Joo, T., Slade, J. H., Shepson, P. B., Ng, N. L., and Gentner, D. R.: Nontargeted Tandem Mass Spectrometry Analysis Reveals Diversity and Variability in Aerosol Functional Groups across Multiple Sites, Seasons, and Times of Day, *Environ. Sci. Technol. Lett.*, 7, 60–69, <https://doi.org/10.1021/acs.estlett.9b00702>, 2020.
- Dou, J., Lin, P., Kuang, B.-Y., and Yu, J. Z.: Reactive Oxygen Species Production Mediated by Humic-like Substances in Atmospheric Aerosols: Enhancement Effects by Pyridine, Imidazole, and Their Derivatives, *Environ. Sci. Technol.*, 49, 6457–6465, <https://doi.org/10.1021/es5059378>, 2015.
- Duan, J., Huang, R. J., Li, Y., Chen, Q., Zheng, Y., Chen, Y., Lin, C., Ni, H., Wang, M., Ovadnevaite, J., Ceburnis, D., Chen, C., Worsnop, D. R., Hoffmann, T., O'Dowd, C., and Cao, J.: Summertime and wintertime atmospheric processes of secondary aerosol in Beijing, *Atmos. Chem. Phys.*, 20, 3793–3807, <https://doi.org/10.5194/acp-20-3793-2020>, 2020.
- Ehhalt, D. H. and Rohrer, F.: Dependence of the OH concentration on solar UV, *J. Geophys. Res.-Atmos.*, 105, 3565–3571, <https://doi.org/10.1029/1999JD901070>, 2000.
- Franze, T., Weller, M. G., Niessner, R., and Pöschl, U.: Protein Nitration by Polluted Air, *Environ. Sci. Technol.*, 39, 1673–1678, <https://doi.org/10.1021/es0488737>, 2005.
- Frege, C., Ortega, I. K., Rissanen, M. P., Praplan, A. P., Steiner, G., Heinritzi, M., Ahonen, L., Amorim, A., Bernhammer, A. K., Bianchi, F., Brilke, S., Breitenlechner, M., Dada, L., Dias, A., Duplissy, J., Ehrhart, S., El-Haddad, I., Fischer, L., Fuchs, C., Garmash, O., Gonin, M., Hansel, A., Hoyle, C. R., Jokinen, T.,

- Junninen, H., Kirkby, J., Kürten, A., Lehtipalo, K., Leiminger, M., Mauldin, R. L., Molteni, U., Nichman, L., Petäjä, T., Sarnela, N., Schobesberger, S., Simon, M., Sipilä, M., Stolzenburg, D., Tomé, A., Vogel, A. L., Wagner, A. C., Wagner, R., Xiao, M., Yan, C., Ye, P., Curtius, J., Donahue, N. M., Flagan, R. C., Kulmala, M., Worsnop, D. R., Winkler, P. M., Dommen, J., and Baltensperger, U.: Influence of temperature on the molecular composition of ions and charged clusters during pure biogenic nucleation, *Atmos. Chem. Phys.*, 18, 65–79, <https://doi.org/10.5194/acp-18-65-2018>, 2018.
- Guo, H., Xu, L., Bougiatioti, A., Cerully, K. M., Capps, S. L., Hite Jr., J. R., Carlton, A. G., Lee, S. H., Bergin, M. H., Ng, N. L., Nenes, A., and Weber, R. J.: Fine-particle water and pH in the southeastern United States, *Atmos. Chem. Phys.*, 15, 5211–5228, <https://doi.org/10.5194/acp-15-5211-2015>, 2015.
- Han, Y., Zhang, X., Li, L., Lin, Y., Zhu, C., Zhang, N., Wang, Q., and Cao, J.: Enhanced Production of Organosulfur Species during a Severe Winter Haze Episode in the Guanzhong Basin of Northwest China, *Environ. Sci. Technol.*, <https://doi.org/10.1021/acs.est.3c02914>, in press, 2023.
- Harrison, M. A. J., Barra, S., Borghesi, D., Vione, D., Arsene, C., and Iulian Olariu, R.: Nitrated phenols in the atmosphere: a review, *Atmos. Environ.*, 39, 231–248, <https://doi.org/10.1016/j.atmosenv.2004.09.044>, 2005.
- Hogg, R. W. and Gillan, F. T.: Fatty acids, sterols and hydrocarbons in the leaves from eleven species of mangrove, *Phytochemistry*, 23, 93–97, [https://doi.org/10.1016/0031-9422\(84\)83084-8](https://doi.org/10.1016/0031-9422(84)83084-8), 1984.
- Iinuma, Y., Böge, O., Gräfe, R., and Herrmann, H.: Methyl-Nitrocatechols: Atmospheric Tracer Compounds for Biomass Burning Secondary Organic Aerosols, *Environ. Sci. Technol.*, 44, 8453–8459, <https://doi.org/10.1021/es102938a>, 2010.
- Jian, Q., Boyer, T. H., Yang, X., Xia, B., and Yang, X.: Characteristics and DBP formation of dissolved organic matter from leachates of fresh and aged leaf litter, *Chemosphere*, 152, 335–344, <https://doi.org/10.1016/j.chemosphere.2016.02.107>, 2016.
- Jiang, H., Li, J., Tang, J., Zhao, S., Chen, Y., Tian, C., Zhang, X., Jiang, B., Liao, Y., and Zhang, G.: Factors Influencing the Molecular Compositions and Distributions of Atmospheric Nitrogen-Containing Compounds, *J. Geophys. Res.-Atmos.*, 127, e2021JD036284, <https://doi.org/10.1029/2021JD036284>, 2022.
- Kenagy, H. S., Romer Present, P. S., Wooldridge, P. J., Nault, B. A., Campuzano-Jost, P., Day, D. A., Jimenez, J. L., Zare, A., Pye, H. O. T., Yu, J., Song, C. H., Blake, D. R., Woo, J.-H., Kim, Y., and Cohen, R. C.: Contribution of Organic Nitrates to Organic Aerosol over South Korea during KORUS-AQ, *Environ. Sci. Technol.*, 55, 16326–16338, <https://doi.org/10.1021/acs.est.1c05521>, 2021.
- Koch, B. P. and Dittmar, T.: From mass to structure: an aromaticity index for high-resolution mass data of natural organic matter, *Rapid Commun. Mass Spectrom.*, 20, 926–932, <https://doi.org/10.1002/rcm.2386>, 2006.
- Kondo, Y., Miyazaki, Y., Takegawa, N., Miyakawa, T., Weber, R. J., Jimenez, J. L., Zhang, Q., and Worsnop, D. R.: Oxygenated and water-soluble organic aerosols in Tokyo, *J. Geophys. Res.-Atmos.*, 112, D01203, <https://doi.org/10.1029/2006JD007056>, 2007.
- Kourtchev, I., Godoi, R. H. M., Connors, S., Levine, J. G., Archibald, A. T., Godoi, A. F. L., Paralovo, S. L., Barbosa, C. G. G., Souza, R. A. F., Manzi, A. O., Seco, R., Sjostedt, S., Park, J. H., Guenther, A., Kim, S., Smith, J., Martin, S. T., and Kalberer, M.: Molecular composition of organic aerosols in central Amazonia: an ultra-high-resolution mass spectrometry study, *Atmos. Chem. Phys.*, 16, 11899–11913, <https://doi.org/10.5194/acp-16-11899-2016>, 2016.
- Kroll, J. H., Donahue, N. M., Jimenez, J. L., Kessler, S. H., Canagaratna, M. R., Wilson, K. R., Altieri, K. E., Mazzoleni, L. R., Wozniak, A. S., Bluhm, H., Mysak, E. R., Smith, J. D., Kolb, C. E., and Worsnop, D. R.: Carbon oxidation state as a metric for describing the chemistry of atmospheric organic aerosol, *Nat. Chem.*, 3, 133–139, <https://doi.org/10.1038/nchem.948>, 2011.
- Laskin, A., Smith, J. S., and Laskin, J.: Molecular Characterization of Nitrogen-Containing Organic Compounds in Biomass Burning Aerosols Using High-Resolution Mass Spectrometry, *Environ. Sci. Technol.*, 43, 3764–3771, <https://doi.org/10.1021/es803456n>, 2009.
- Laskin, J., Laskin, A., Nizkorodov, S. A., Roach, P., Eckert, P., Gilles, M. K., Wang, B., Lee, H. J., and Hu, Q.: Molecular Selectivity of Brown Carbon Chromophores, *Environ. Sci. Technol.*, 48, 12047–12055, <https://doi.org/10.1021/es503432r>, 2014.
- Lee, B. H., Mohr, C., Lopez-Hilfiker, F. D., Lutz, A., Hallquist, M., Lee, L., Romer, P., Cohen, R. C., Iyer, S., Kurtén, T., Hu, W., Day, D. A., Campuzano-Jost, P., Jimenez, J. L., Xu, L., Ng, N. L., Guo, H., Weber, R. J., Wild, R. J., Brown, S. S., Koss, A., de Gouw, J., Olson, K., Goldstein, A. H., Seco, R., Kim, S., McAvey, K., Shepson, P. B., Starn, T., Baumann, K., Edgerton, E. S., Liu, J., Shilling, J. E., Miller, D. O., Brune, W., Schobesberger, S., D'Ambro, E. L., and Thornton, J. A.: Highly functionalized organic nitrates in the southeast United States: Contribution to secondary organic aerosol and reactive nitrogen budgets, *P. Natl. Acad. Sci. USA*, 113, 1516–1521, <https://doi.org/10.1073/pnas.1508108113>, 2016.
- Li, S., Liu, D., Kong, S., Wu, Y., Hu, K., Zheng, H., Cheng, Y., Zheng, S., Jiang, X., Ding, S., Hu, D., Liu, Q., Tian, P., Zhao, D., and Sheng, J.: Evolution of source attributed organic aerosols and gases in a megacity of central China, *Atmos. Chem. Phys.*, 22, 6937–6951, <https://doi.org/10.5194/acp-22-6937-2022>, 2022.
- Li, Y., Chen, M., Wang, Y., Huang, T., Wang, G., Li, Z., Li, J., Meng, J., and Hou, Z.: Seasonal characteristics and provenance of organic aerosols in the urban atmosphere of Liaocheng in the North China Plain: Significant effect of biomass burning, *Particuology*, 75, 185–198, <https://doi.org/10.1016/j.partic.2022.07.012>, 2023.
- Lin, P., Rincon, A. G., Kalberer, M., and Yu, J. Z.: Elemental Composition of HULIS in the Pearl River Delta Region, China: Results Inferred from Positive and Negative Electrospray High Resolution Mass Spectrometric Data, *Environ. Sci. Technol.*, 46, 7454–7462, <https://doi.org/10.1021/es300285d>, 2012.
- Lin, X., Xu, Y., Zhu, R.-G., Xiao, H.-W., and Xiao, H.-Y.: Proteinaceous Matter in PM_{2.5} in Suburban Guiyang, Southwestern China: Decreased Importance in Long-Range Transport and Atmospheric Degradation, *J. Geophys. Res.-Atmos.*, 128, e2023JD038516, <https://doi.org/10.1029/2023JD038516>, 2023.
- Liu, T., Hong, Y., Li, M., Xu, L., Chen, J., Bian, Y., Yang, C., Dan, Y., Zhang, Y., Xue, L., Zhao, M., Huang, Z., and Wang, H.: Atmospheric oxidation capacity and ozone pollution mech-

- anism in a coastal city of southeastern China: analysis of a typical photochemical episode by an observation-based model, *Atmos. Chem. Phys.*, 22, 2173–2190, <https://doi.org/10.5194/acp-22-2173-2022>, 2022.
- Liu, T., Xu, Y., Sun, Q.-B., Xiao, H.-W., Zhu, R.-G., Li, C.-X., Li, Z.-Y., Zhang, K.-Q., Sun, C.-X., and Xiao, H.-Y.: Characteristics, Origins, and Atmospheric Processes of Amines in Fine Aerosol Particles in Winter in China, *J. Geophys. Res.-Atmos.*, 128, e2023JD038974, <https://doi.org/10.1029/2023JD038974>, 2023.
- Ma, L., Guzman, C., Niedek, C., Tran, T., Zhang, Q., and Anastasio, C.: Kinetics and Mass Yields of Aqueous Secondary Organic Aerosol from Highly Substituted Phenols Reacting with a Triplet Excited State, *Environ. Sci. Technol.*, 55, 5772–5781, <https://doi.org/10.1021/acs.est.1c00575>, 2021.
- Ma, Y. J., Xu, Y., Yang, T., Xiao, H. W., and Xiao, H. Y.: Characteristics of nitrogen-containing organics in PM_{2.5} in Ürümqi, northwestern China – differential impacts of combustion of fresh and aged biomass materials, Zenodo [data set], <https://doi.org/10.5281/zenodo.10453929>, 2024.
- Merder, J., Freund, J. A., Feudel, U., Hansen, C. T., Hawkes, J. A., Jacob, B., Klapproth, K., Niggemann, J., Noriega-Ortega, B. E., Osterholz, H., Rossel, P. E., Seidel, M., Singer, G., Stubbins, A., Waska, H., and Dittmar, T.: ICBM-OCEAN: Processing Ultrahigh-Resolution Mass Spectrometry Data of Complex Molecular Mixtures, *Anal. Chem.*, 92, 6832–6838, <https://doi.org/10.1021/acs.analchem.9b05659>, 2020.
- Nguyen, T. B., Bates, K. H., Crouse, J. D., Schwantes, R. H., Zhang, X., Kjaergaard, H. G., Surratt, J. D., Lin, P., Laskin, A., Seinfeld, J. H., and Wennberg, P. O.: Mechanism of the hydroxyl radical oxidation of methacryloyl peroxyoxynitrate (MPAN) and its pathway toward secondary organic aerosol formation in the atmosphere, *Phys. Chem. Chem. Phys.*, 17, 17914–17926, <https://doi.org/10.1039/C5CP02001H>, 2015.
- Perring, A. E., Pusede, S. E., and Cohen, R. C.: An Observational Perspective on the Atmospheric Impacts of Alkyl and Multifunctional Nitrates on Ozone and Secondary Organic Aerosol, *Chem. Rev.*, 113, 5848–5870, <https://doi.org/10.1021/cr300520x>, 2013.
- Qiu, C. and Zhang, R.: Multiphase chemistry of atmospheric amines, *Phys. Chem. Chem. Phys.*, 15, 5738–5752, <https://doi.org/10.1039/C3CP43446j>, 2013.
- Qizhi, M., Ying, L., Kang, W., and Qingfei, Z.: Spatio-Temporal Changes of Population Density and Urbanization Pattern in China (2000–2010), *China City Plan. Rev.*, 25, 8–14, 2016.
- Radzi Bin Abas, M., Rahman, N. A., Omar, N. Y. M. J., Maah, M. J., Abu Samah, A., Oros, D. R., Otto, A., and Simoneit, B. R. T.: Organic composition of aerosol particulate matter during a haze episode in Kuala Lumpur, Malaysia, *Atmos. Environ.*, 38, 4223–4241, <https://doi.org/10.1016/j.atmosenv.2004.01.048>, 2004.
- Ren, Y., Wang, G., Wu, C., Wang, J., Li, J., Zhang, L., Han, Y., Liu, L., Cao, C., Cao, J., He, Q., and Liu, X.: Changes in concentration, composition and source contribution of atmospheric organic aerosols by shifting coal to natural gas in Urumqi, *Atmos. Environ.*, 148, 306–315, <https://doi.org/10.1016/j.atmosenv.2016.10.053>, 2017.
- Rollins, A. W., Browne, E. C., Min, K.-E., Pusede, S. E., Wooldridge, P. J., Gentner, D. R., Goldstein, A. H., Liu, S., Day, D. A., Russell, L. M., and Cohen, R. C.: Evidence for NO_x Control over Nighttime SOA Formation, *Science*, 337, 1210–1212, <https://doi.org/10.1126/science.1221520>, 2012.
- Salvador, C. M. G., Tang, R., Priestley, M., Li, L., Tsiligiannis, E., Le Breton, M., Zhu, W., Zeng, L., Wang, H., Yu, Y., Hu, M., Guo, S., and Hallquist, M.: Ambient nitro-aromatic compounds – biomass burning versus secondary formation in rural China, *Atmos. Chem. Phys.*, 21, 1389–1406, <https://doi.org/10.5194/acp-21-1389-2021>, 2021.
- Samy, S. and Hays, M. D.: Quantitative LC–MS for water-soluble heterocyclic amines in fine aerosols (PM_{2.5}) at Duke Forest, USA, *Atmos. Environ.*, 72, 77–80, <https://doi.org/10.1016/j.atmosenv.2013.02.032>, 2013.
- Schauer, J. J., Kleeman, M. J., Cass, G. R., and Simoneit, B. R. T.: Measurement of Emissions from Air Pollution Sources. 1. C₁ through C₂₉ Organic Compounds from Meat Charbroiling, *Environ. Sci. Technol.*, 33, 1566–1577, <https://doi.org/10.1021/es980076j>, 1999.
- Seinfeld, J. H., Bretherton, C., Carslaw, K. S., Coe, H., DeMott, P. J., Dunlea, E. J., Feingold, G., Ghan, S., Guenther, A. B., Kahn, R., Kraucunas, I., Kreidenweis, S. M., Molina, M. J., Nenes, A., Penner, J. E., Prather, K. A., Ramanathan, V., Ramaswamy, V., Rasch, P. J., Ravishankara, A. R., Rosenfeld, D., Stephens, G., and Wood, R.: Improving our fundamental understanding of the role of aerosol-cloud interactions in the climate system, *P. Natl. Acad. Sci. USA*, 113, 5781–5790, <https://doi.org/10.1073/pnas.1514043113>, 2016.
- Simoneit, B. R. T., Rushdi, A. I., bin Abas, M. R., and Didyk, B. M.: Alkyl Amides and Nitriles as Novel Tracers for Biomass Burning, *Environ. Sci. Technol.*, 37, 16–21, <https://doi.org/10.1021/es020811y>, 2003.
- Smith, J. D., Sio, V., Yu, L., Zhang, Q., and Anastasio, C.: Secondary Organic Aerosol Production from Aqueous Reactions of Atmospheric Phenols with an Organic Triplet Excited State, *Environ. Sci. Technol.*, 48, 1049–1057, <https://doi.org/10.1021/es4045715>, 2014.
- Song, J., Li, M., Jiang, B., Wei, S., Fan, X., and Peng, P. A.: Molecular Characterization of Water-Soluble Humic like Substances in Smoke Particles Emitted from Combustion of Biomass Materials and Coal Using Ultrahigh-Resolution Electrospray Ionization Fourier Transform Ion Cyclotron Resonance Mass Spectrometry, *Environ. Sci. Technol.*, 52, 2575–2585, <https://doi.org/10.1021/acs.est.7b06126>, 2018.
- Song, J., Li, M., Zou, C., Cao, T., Fan, X., Jiang, B., Yu, Z., Jia, W., and Peng, P. A.: Molecular Characterization of Nitrogen-Containing Compounds in Humic-like Substances Emitted from Biomass Burning and Coal Combustion, *Environ. Sci. Technol.*, 56, 119–130, <https://doi.org/10.1021/acs.est.1c04451>, 2022.
- Stolzenburg, D., Fischer, L., Vogel, A. L., Heinritzi, M., Schervish, M., Simon, M., Wagner, A. C., Dada, L., Ahonen, L. R., Amorim, A., Baccarini, A., Bauer, P. S., Baumgartner, B., Bergen, A., Bianchi, F., Breitenlechner, M., Brilke, S., Buenrostro Mazon, S., Chen, D., Dias, A., Draper, D. C., Duplissy, J., El Haddad, I., Finkenzeller, H., Frege, C., Fuchs, C., Garmash, O., Gordon, H., He, X., Helm, J., Hofbauer, V., Hoyle, C. R., Kim, C., Kirkby, J., Kontkanen, J., Kürten, A., Lampilahti, J., Lawler, M., Lehtipalo, K., Leiminger, M., Mai, H., Mathot, S., Mentler, B., Molteni, U., Nie, W., Nieminen, T., Nowak, J. B., Ojdanic, A., Onnela, A., Passananti, M., Petäjä, T., Quéléver, L. L. J., Rissanen, M. P., Sarnela, N., Schallhart, S., Tauber, C., Tomé, A., Wagner, R., Wang, M., Weitz, L., Wimmer, D., Xiao, M., Yan, C., Ye, P., Zha, Q., Baltensperger, U., Curtius, J., Dom-

- men, J., Flagan, R. C., Kulmala, M., Smith, J. N., Worsnop, D. R., Hansel, A., Donahue, N. M., and Winkler, P. M.: Rapid growth of organic aerosol nanoparticles over a wide tropospheric temperature range, *P. Natl. Acad. Sci. USA*, 115, 9122–9127, <https://doi.org/10.1073/pnas.1807604115>, 2018.
- Su, S., Xie, Q., Lang, Y., Cao, D., Xu, Y., Chen, J., Chen, S., Hu, W., Qi, Y., Pan, X., Sun, Y., Wang, Z., Liu, C.-Q., Jiang, G., and Fu, P.: High Molecular Diversity of Organic Nitrogen in Urban Snow in North China, *Environ. Sci. Technol.*, 55, 4344–4356, <https://doi.org/10.1021/acs.est.0c06851>, 2021.
- Surratt, J. D., Chan, A. W. H., Eddingsaas, N. C., Chan, M., Loza, C. L., Kwan, A. J., Hersey, S. P., Flagan, R. C., Wennberg, P. O., and Seinfeld, J. H.: Reactive intermediates revealed in secondary organic aerosol formation from isoprene, *P. Natl. Acad. Sci. USA*, 107, 6640–6645, <https://doi.org/10.1073/pnas.0911114107>, 2010.
- Tomsche, L., Piel, F., Mikoviny, T., Nielsen, C. J., Guo, H., Campuzano-Jost, P., Nault, B. A., Schueneman, M. K., Jimenez, J. L., Halliday, H., Diskin, G., DiGangi, J. P., Nowak, J. B., Wiggins, E. B., Gargulinski, E., Soja, A. J., and Wisthaler, A.: Measurement report: Emission factors of NH₃ and NH_x for wildfires and agricultural fires in the United States, *Atmos. Chem. Phys.*, 23, 2331–2343, <https://doi.org/10.5194/acp-23-2331-2023>, 2023.
- Wan, X., Qin, F., Cui, F., Chen, W., Ding, H., and Li, C.: Correlation between the distribution of solar energy resources and the cloud cover in Xinjiang, *IOP Conf. Ser.: Earth Environ. Sci.*, 675, 012060, <https://doi.org/10.1088/1755-1315/675/1/012060>, 2021.
- Wang, H., Wang, Q., Gao, Y., Zhou, M., Jing, S., Qiao, L., Yuan, B., Huang, D., Huang, C., Lou, S., Yan, R., de Gouw, J. A., Zhang, X., Chen, J., Chen, C., Tao, S., An, J., and Li, Y.: Estimation of Secondary Organic Aerosol Formation During a Photochemical Smog Episode in Shanghai, China, *J. Geophys. Res.-Atmos.*, 125, e2019JD032033, <https://doi.org/10.1029/2019JD032033>, 2020.
- Wang, K., Huang, R.-J., Brueggemann, M., Zhang, Y., Yang, L., Ni, H., Guo, J., Wang, M., Han, J., Bilde, M., Glasius, M., and Hoffmann, T.: Urban organic aerosol composition in eastern China differs from north to south: molecular insight from a liquid chromatography-mass spectrometry (Orbitrap) study, *Atmos. Chem. Phys.*, 21, 9089–9104, <https://doi.org/10.5194/acp-21-9089-2021>, 2021.
- Wang, L., Zhang, K., Huang, W., Han, W., and Tian, C.-Y.: Seed oil content and fatty acid composition of annual halophyte *Suaeda acuminata*: A comparative study on dimorphic seeds, *Afr. J. Biotechnol.*, 10, 19106–19108, <https://doi.org/10.5897/ajb11.2597>, 2011.
- Wang, Q., Shao, M., Zhang, Y., Wei, Y., Hu, M., and Guo, S.: Source apportionment of fine organic aerosols in Beijing, *Atmos. Chem. Phys.*, 9, 8573–8585, <https://doi.org/10.5194/acp-9-8573-2009>, 2009.
- Wang, X., Hayeck, N., Brüggemann, M., Yao, L., Chen, H., Zhang, C., Emmelin, C., Chen, J., George, C., and Wang, L.: Chemical Characteristics of Organic Aerosols in Shanghai: A Study by Ultrahigh-Performance Liquid Chromatography Coupled With Orbitrap Mass Spectrometry, *J. Geophys. Res.-Atmos.*, 122, 11703–11722, <https://doi.org/10.1002/2017JD026930>, 2017.
- Wang, X., Shen, Z., Liu, F., Lu, D., Tao, J., Lei, Y., Zhang, Q., Zeng, Y., Xu, H., Wu, Y., Zhang, R., and Cao, J.: Saccharides in summer and winter PM_{2.5} over Xi'an, North-western China: Sources, and yearly variations of biomass burning contribution to PM_{2.5}, *Atmos. Res.*, 214, 410–417, <https://doi.org/10.1016/j.atmosres.2018.08.024>, 2018.
- Wang, Y., Hu, M., Lin, P., Guo, Q., Wu, Z., Li, M., Zeng, L., Song, Y., Zeng, L., Wu, Y., Guo, S., Huang, X., and He, L.: Molecular Characterization of Nitrogen-Containing Organic Compounds in Humic-like Substances Emitted from Straw Residue Burning, *Environ. Sci. Technol.*, 51, 5951–5961, <https://doi.org/10.1021/acs.est.7b00248>, 2017.
- Wang, Y., Zhao, Y., Li, Z., Li, C., Yan, N., and Xiao, H.: Importance of Hydroxyl Radical Chemistry in Isoprene Suppression of Particle Formation from α -Pinene Ozonolysis, *ACS Earth Space Chem.*, 5, 487–499, <https://doi.org/10.1021/acsearthspacechem.0c00294>, 2021a.
- Wang, Y., Hu, M., Hu, W., Zheng, J., Niu, H., Fang, X., Xu, N., Wu, Z., Guo, S., Wu, Y., Chen, W., Lu, S., Shao, M., Xie, S., Luo, B., and Zhang, Y.: Secondary Formation of Aerosols Under Typical High-Humidity Conditions in Wintertime Sichuan Basin, China: A Contrast to the North China Plain, *J. Geophys. Res.-Atmos.*, 126, e2021JD034560, <https://doi.org/10.1029/2021JD034560>, 2021b.
- Xie, Q., Su, S., Chen, S., Xu, Y., Cao, D., Chen, J., Ren, L., Yue, S., Zhao, W., Sun, Y., Wang, Z., Tong, H., Su, H., Cheng, Y., Kawamura, K., Jiang, G., Liu, C. Q., and Fu, P.: Molecular characterization of firework-related urban aerosols using Fourier transform ion cyclotron resonance mass spectrometry, *Atmos. Chem. Phys.*, 20, 6803–6820, <https://doi.org/10.5194/acp-20-6803-2020>, 2020.
- Xu, Y. and Xiao, H.: Concentrations and nitrogen isotope compositions of free amino acids in *Pinus massoniana* (Lamb.) needles of different ages as indicators of atmospheric nitrogen pollution, *Atmos. Environ.*, 164, 348–359, <https://doi.org/10.1016/j.atmosenv.2017.06.024>, 2017.
- Xu, Y., Miyazaki, Y., Tachibana, E., Sato, K., Ramasamy, S., Mochizuki, T., Sadanaga, Y., Nakashima, Y., Sakamoto, Y., Matsuda, K., and Kajii, Y.: Aerosol Liquid Water Promotes the Formation of Water-Soluble Organic Nitrogen in Submicrometer Aerosols in a Suburban Forest, *Environ. Sci. Technol.*, 54, 1406–1414, <https://doi.org/10.1021/acs.est.9b05849>, 2020.
- Xu, Y., Lin, Z., and Wu, C.: Spatiotemporal Variation of the Burned Area and Its Relationship with Climatic Factors in Central Kazakhstan, *Remote Sens.*, 13, 313, <https://doi.org/10.3390/rs13020313>, 2021.
- Xu, Y., Dong, X.-N., Xiao, H.-Y., He, C., and Wu, D.-S.: Water-Insoluble Components in Rainwater in Suburban Guiyang, Southwestern China: A Potential Contributor to Dissolved Organic Carbon, *J. Geophys. Res.-Atmos.*, 127, e2022JD037721, <https://doi.org/10.1029/2022JD037721>, 2022a.
- Xu, Y., Dong, X.-N., Xiao, H.-Y., Zhou, J.-X., and Wu, D.-S.: Proteinaceous Matter and Liquid Water in Fine Aerosols in Nanchang, Eastern China: Seasonal Variations, Sources, and Potential Connections, *J. Geophys. Res.-Atmos.*, 127, e2022JD036589, <https://doi.org/10.1029/2022JD036589>, 2022b.
- Xu, Y., Dong, X. N., He, C., Wu, D. S., Xiao, H. W., and Xiao, H. Y.: Mist cannon trucks can exacerbate the formation of water-soluble organic aerosol and PM_{2.5} pollution in the road environment, *Atmos. Chem. Phys.*, 23, 6775–6788, <https://doi.org/10.5194/acp-23-6775-2023>, 2023.

- Yang, T., Xu, Y., Ye, Q., Ma, Y. J., Wang, Y. C., Yu, J. Z., Duan, Y. S., Li, C. X., Xiao, H. W., Li, Z. Y., Zhao, Y., and Xiao, H. Y.: Spatial and diurnal variations of aerosol organosulfates in summertime Shanghai, China: potential influence of photochemical processes and anthropogenic sulfate pollution, *Atmos. Chem. Phys.*, 23, 13433–13450, <https://doi.org/10.5194/acp-23-13433-2023>, 2023.
- Zahardis, J., Geddes, S., and Petrucci, G. A.: The ozonolysis of primary aliphatic amines in fine particles, *Atmos. Chem. Phys.*, 8, 1181–1194, <https://doi.org/10.5194/acp-8-1181-2008>, 2008.
- Zarzana, K. J., De Haan, D. O., Freedman, M. A., Hasenkopf, C. A., and Tolbert, M. A.: Optical Properties of the Products of α -Dicarbonyl and Amine Reactions in Simulated Cloud Droplets, *Environ. Sci. Technol.*, 46, 4845–4851, <https://doi.org/10.1021/es2040152>, 2012.
- Zeng, Y., Shen, Z., Takahama, S., Zhang, L., Zhang, T., Lei, Y., Zhang, Q., Xu, H., Ning, Y., Huang, Y., Cao, J., and Rudolf, H.: Molecular Absorption and Evolution Mechanisms of PM_{2.5} Brown Carbon Revealed by Electrospray Ionization Fourier Transform–Ion Cyclotron Resonance Mass Spectrometry During a Severe Winter Pollution Episode in Xi'an, China, *Geophys. Res. Lett.*, 47, e2020GL087977, <https://doi.org/10.1029/2020GL087977>, 2020.
- Zeng, Y., Ning, Y., Shen, Z., Zhang, L., Zhang, T., Lei, Y., Zhang, Q., Li, G., Xu, H., Ho, S. S. H., and Cao, J.: The Roles of N, S, and O in Molecular Absorption Features of Brown Carbon in PM_{2.5} in a Typical Semi-Arid Megacity in Northwestern China, *J. Geophys. Res.-Atmos.*, 126, e2021JD034791, <https://doi.org/10.1029/2021JD034791>, 2021.
- Zhang, B., Shen, Z., He, K., Sun, J., Huang, S., Xu, H., Li, J., Ho, S. S. H., and Cao, J.-J.: Insight into the Primary and Secondary Particle-Bound Methoxyphenols and Nitroaromatic Compound Emissions from Solid Fuel Combustion and the Updated Source Tracers, *Environ. Sci. Technol.*, 57, 14280–14288, <https://doi.org/10.1021/acs.est.3c04370>, 2023.
- Zhang, Q., Jimenez, J. L., Canagaratna, M. R., Allan, J. D., Coe, H., Ulbrich, I., Alfarra, M. R., Takami, A., Middlebrook, A. M., Sun, Y. L., Dzepina, K., Dunlea, E., Docherty, K., DeCarlo, P. F., Salcedo, D., Onasch, T., Jayne, J. T., Miyoshi, T., Shimojo, A., Hatakeyama, S., Takegawa, N., Kondo, Y., Schneider, J., Drewnick, F., Borrmann, S., Weimer, S., Demerjian, K., Williams, P., Bower, K., Bahreini, R., Cottrell, L., Griffin, R. J., Rautiainen, J., Sun, J. Y., Zhang, Y. M., and Worsnop, D. R.: Ubiquity and dominance of oxygenated species in organic aerosols in anthropogenically-influenced Northern Hemisphere midlatitudes, *Geophys. Res. Lett.*, 34, L13801, <https://doi.org/10.1029/2007GL029979>, 2007.
- Zhang, T., Shen, Z., Huang, S., Lei, Y., Zeng, Y., Sun, J., Zhang, Q., Ho, S. S. H., Xu, H., and Cao, J.: Optical properties, molecular characterizations, and oxidative potentials of different polarity levels of water-soluble organic matters in winter PM_{2.5} in six China's megacities, *Sci. Total Environ.*, 853, 158600, <https://doi.org/10.1016/j.scitotenv.2022.158600>, 2022.
- Zhao, Y., Hu, M., Slanina, S., and Zhang, Y.: Chemical Compositions of Fine Particulate Organic Matter Emitted from Chinese Cooking, *Environ. Sci. Technol.*, 41, 99–105, <https://doi.org/10.1021/es0614518>, 2007.
- Zhong, S., Chen, S., Deng, J., Fan, Y., Zhang, Q., Xie, Q., Qi, Y., Hu, W., Wu, L., Li, X., Pavuluri, C. M., Zhu, J., Wang, X., Liu, D., Pan, X., Sun, Y., Wang, Z., Xu, Y., Tong, H., Su, H., Cheng, Y., Kawamura, K., and Fu, P.: Impact of biogenic secondary organic aerosol (SOA) loading on the molecular composition of wintertime PM_{2.5} in urban Tianjin: an insight from Fourier transform ion cyclotron resonance mass spectrometry, *Atmos. Chem. Phys.*, 23, 2061–2077, <https://doi.org/10.5194/acp-23-2061-2023>, 2023.
- Zhou, S., Guo, F., Chao, C.-Y., Yoon, S., Alvarez, S. L., Shrestha, S., Flynn III, J. H., Usenko, S., Sheesley, R. J., and Griffin, R. J.: Marine Submicron Aerosols from the Gulf of Mexico: Polluted and Acidic with Rapid Production of Sulfate and Organosulfates, *Environ. Sci. Technol.*, 57, 5149–5159, <https://doi.org/10.1021/acs.est.2c05469>, 2023.
- Zou, C., Cao, T., Li, M., Song, J., Jiang, B., Jia, W., Li, J., Ding, X., Yu, Z., Zhang, G., and Peng, P.: Measurement report: Changes in light absorption and molecular composition of water-soluble humic-like substances during a winter haze bloom-decay process in Guangzhou, China, *Atmos. Chem. Phys.*, 23, 963–979, <https://doi.org/10.5194/acp-23-963-2023>, 2023.